they decay very rapidly in the direction of increasing and decreasing $\tilde{S}_2$. The molecules are thus shown to be highly anisometric.

It is also clear from Figures 2b and 4b that the most probable configurations for both circular and linear chains are very compact. Circular chains are likely to have smaller dimensions than linear ones. For example, the principal components of the gyration tensor for circular chains are 70% and 83% of those for linear chains at the most probable configuration of each. For disks, the most probable configuration for the circular chain is 80% as large as that for the linear chain. In the highly extended region, the circular chain is shown to be wider than the linear. For the most probable configurations, the ratio of the two principal components for the linear chains is found to be 2.66:1. It is of interest to compare this result with averaged dimensions found by Šolc[4] for Monte Carlo generated lattice chains. In this case, it was found that $\langle S_1\rangle:\langle S_2\rangle:\langle S_3\rangle \simeq 11.7:2.7:1$. The close similarity between the ratio of most probable components for the two-dimensional linear chain and the two smaller averaged components for the three-dimensional one suggests that their distribution functions behave similarly and that fluctuations for three-dimensional chains will also be quasi-uniaxial.

The distribution function of the gyration tensor varies rapidly with the chain length for short chains, but it reaches the large n limit quickly. In two dimensions, chains with $n = 49$ beads are virtually at the asymptotic $n \rightarrow \infty$ limit.

Acknowledgment. This work was supported by the Department of Energy, Grant DE-FG06-84ER45123.

References and Notes

(1) Fixman, M. *J. Chem. Phys.* **1962**, *36*, 306.
(2) Fujita, H.; Norisuye, T. *J. Chem. Phys.* **1970**, *52*, 1115.
(3) Gupta, S. K.; Forsman, W. C. *J. Chem. Phys.* **1976**, *65*, 201.
(4) Šolc, K. *J. Chem. Phys.* **1971**, *55*, 335.
(5) Mattice, W. *Macromolecules* **1981**, *14*, 863.
(6) Rubin, R. J.; Mazur, J. *Macromolecules* **1977**, *10*, 139.
(7) Theodorou, D. N.; Suter, U. W. *Macromolecules* **1985**, *18*, 1206.
(8) Eichinger, B. E. *Macromolecules* **1985**, *18*, 211.
(9) Šolc, K. *Macromolecules* **1972**, *5*, 705.
(10) Šolc, K.; Gobush, W. *Macromolecules* **1974**, *7*, 814.
(11) Eichinger, B. E *Pure Appl. Chem.* **1975**, *43*, 97.
(12) Eichinger, B. E. *Macromolecules* **1977**, *10*, 671.
(13) Neuburger, N. A.; Eichinger, B. E. *J. Chem. Phys.* **1985**, *83*, 884.
(14) Eichinger, B. E. *Macromolecules* **1980**, *13*, 1.
(15) "The IMSL Library", Reference Manual, 9th ed.; International Mathematical and Statistical Libraries: Houston, TX, 1982; Program DCADRE.
(16) Ahlfors, L. V. "Complex Analysis", 3rd ed.; McGraw-Hill: New York, 1979; Chapter 3.
(17) Abramowitz, M.; Stegun, I. A. "Handbook of Mathematical Functions"; National Bureau of Standards, Applied Math. Sec. 55, 1970, p 879.
(18) Eichinger, B. E.; Martin, J. E. *J. Chem. Phys.* **1978**, *69*, 4588.
(19) Gerald, C. F. "Applied Numerical Analysis", 2nd ed.; Addison Wesley: Readings, MA, 1977, Chapter 4.

Excluded Volume Change Due to Segmental Orientation in Polymer Solutions

A. Sariban

Institut für Physik der Universität Mainz, D-6500 Mainz, Federal Republic of Germany.

Received June 26, 1985

ABSTRACT: The excluded volume effect of macromolecules in the external field, producing a partial orientation of segments, was estimated by a model calculation. The lattice model with non-self-intersections of the monomers and with the interactions between the nearest-neighbor monomers was used. The calculations predict maxima of excluded volume in unoriented systems and a continuous decrease of excluded volume with increase of any kind of segment orientation.

Introduction

When the behavior of macromolecules in dilute solution is studied, the Θ-state, where the repulsive and attractive parts of long-range interactions compensate each other and effectively only short-range interactions between two segments remain, is of great importance. The long-range interaction is described in terms of the "excluded volume" for the statistical segment (v_s) or for the monomer (v_m). At the Θ-point, $v_s = v_m = 0$; i.e., excluded volume effects disappear.[1,2]

Recently, Lindner and Oberthür[3] studied the statistical behavior of the isolated macromolecule in shear gradient by means of neutron scattering. The characteristics of the investigated polymer were measured in the Θ-state of the chosen system. The question as to whether the Θ-state determined in the usual manner for the motionless case remains relevant in a shear gradient initiated this work.

It is only possible to obtain the excluded volume in analytical form for simple rigid bodies such as a sphere, cube, or circular cylinder (see, for example, ref 4, Chapter 5, Table 5.1). For the dumbell model,[5] a rigid body that can be considered a first step toward a "pearl necklace" model of a macromolecule, it is possible to obtain the result only in numerical form. If we are interested not only in a rigid body model with a hard-core potential of interactions but also in the attractive interactions of van der Waals type, the task becomes much more difficult. In the present work we have therefore chosen a very simple model that nevertheless contains all the properties of interest in a simplified form. With the aid of this model we hope to attain qualitatively a general understanding of the influence of the (macro)molecular orientation on the excluded volume effects.

Description of the Model

Our macromolecular model is schematically represented in Figure 1. The infinite macromolecule is placed on the simple cubic lattice. The length of each elementary cell

0024-9297/86/2219-0843$01.50/0 © 1986 American Chemical Society

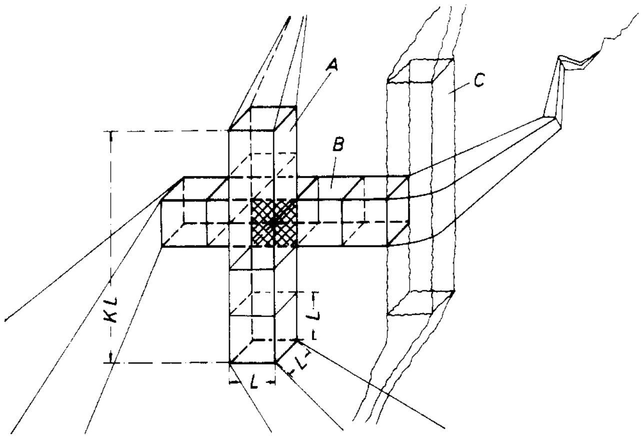

Figure 1. Macromolecular model used in the present work. A, B, and C represent interacting segments belonging to the same infinite molecule.

Table I
Possible Mutual Positions between Two Interacting Rods (See Text)

i		V_s^i/L^3	N_i	
I	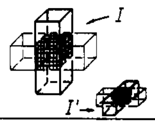	K^2	1 + 1	+
II	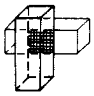	$K^2(1-q)$	2 + 2	+
III	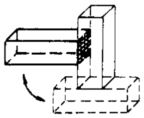	$K(1-q)$	4 + 4	–
IV	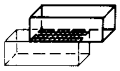	$2K-\frac{(1-q^K)(1+q)}{1-q}$	4	+
V		$2K-1$	1	–
VI		$1-q$	2	–

is L and the volume is L^3. Each monomer in the macromolecule occupies one elementary lattice cell. Each statistical segment consists of K monomers and is a rectangular prism with two short sides L and a long side LK. The segments are attached to one another without any correlations between subsequent segments.

In addition to the present macromolecular model, we consider the analogous simple model for small rod-shaped molecules consisting of K cubes of volume L^3. Intersections of the monomers in our model are prohibited (hard core). A pair of monomers in adjacent lattice sites (excepting the monomers attached to one another in a macromolecular chain or rod) was attributed to the energy parameter ϵ (determined in units kT).

It is convenient to consider the excluded volume of two intersecting monomers in our lattice model as L^3 (volume of one monomer). The contribution to the excluded volume due to interaction of two adjacent monomers is $L^3(1-q)$, where $q = e^{-\epsilon}$.[6]

Table I shows all the possible different mutual positions between two rods giving some contribution to the excluded volume effect of this system. v_s^i/L^3 is just the contribution to the excluded volume of each of these positions (normalized for convenience to L^3), and N is the number of different ways to achieve these positions. The similar positions that can be achieved by different mutual directions of rods are represented as a sum of various contributions. So the excluded volume effect is given by

$$\frac{v_s}{L^3} = \frac{1}{L^3}\sum_{i=\mathrm{I}}^{\mathrm{VI}} v_s^i N_i \tag{1}$$

Table II
Probabilities of Situations Depicted in Table I by Appropriately Directed Rods

	direction of the longer axis		
i	"first" rod	"second" rod	probability
I, II, III	x	y	$\alpha[(1-\alpha)/2]$
		z	$\alpha[(1-\alpha)/2]$
	y	x	$[(1-\alpha)/2]\alpha$
		z	$(1-\alpha)^2/4$
	z	x	$[(1-\alpha)/2]\alpha$
		y	$(1-\alpha)^2/4$
IV, V, VI	x	x	α^2
	y	y	$(1-\alpha)^2/4$
	z	z	$(1-\alpha)^2/4$

The polymer model differs from this simple rod model because in the interaction of two segments of a macromolecule, only some of the positions described in Table I have to be taken into account. This is due to the fact that some of these positions are simultaneously positions for the neighboring rods attached to the given rod. For example, the position of segment C in Figure 1 is position III in Table I for segment B but is simultaneously position I for the next segment connected with segment B. In the last column of Table I positions essential for the "polymer" case are indicated with "+" and those positions giving only a contribution in the "two-rods" model (which have to be omitted in the "polymer" model) are indicated with "–".

Our essential new supposition is in assuming (both for "small molecules" and "macromolecules") that each rod or segment is fully independent of the other rods and is directed with its longest side along a chosen axis (the x axis) with probability α and along the other axes (the y and z axes) with probability $(1-\alpha)/2$. The physical meaning of this assumption is quite clear: the external force effectively acts on each segment independently. If $\alpha = {}^1/_3$ we have the usual situation without any particular direction. The treatment of orientation of rods by assignment of different probabilities along Cartesian axes was used earlier in order to study the phase transitions in ensembles of rods.[7]

In Table II we consider all possible situations for the directions of the long axis of two rods with appropriate probabilities. Counting all these possibilities with appropriate probabilities, we obtain for the "small-molecule" model an expression for the excluded volume:

$$\frac{v_s'}{L^3} = \left[\alpha(1-\alpha) + \frac{1-\alpha^2}{2}\right] \times \{K^2 + 2K^2(1-q) + 4K(1-q)\} + \left[\alpha^2 + \frac{(1-\alpha)^2}{2}\right] \times \left\{8K - \frac{4(1-q^K)(1+q)}{1-q} + (2K-1) + 2(1-q)\right\} \tag{2}$$

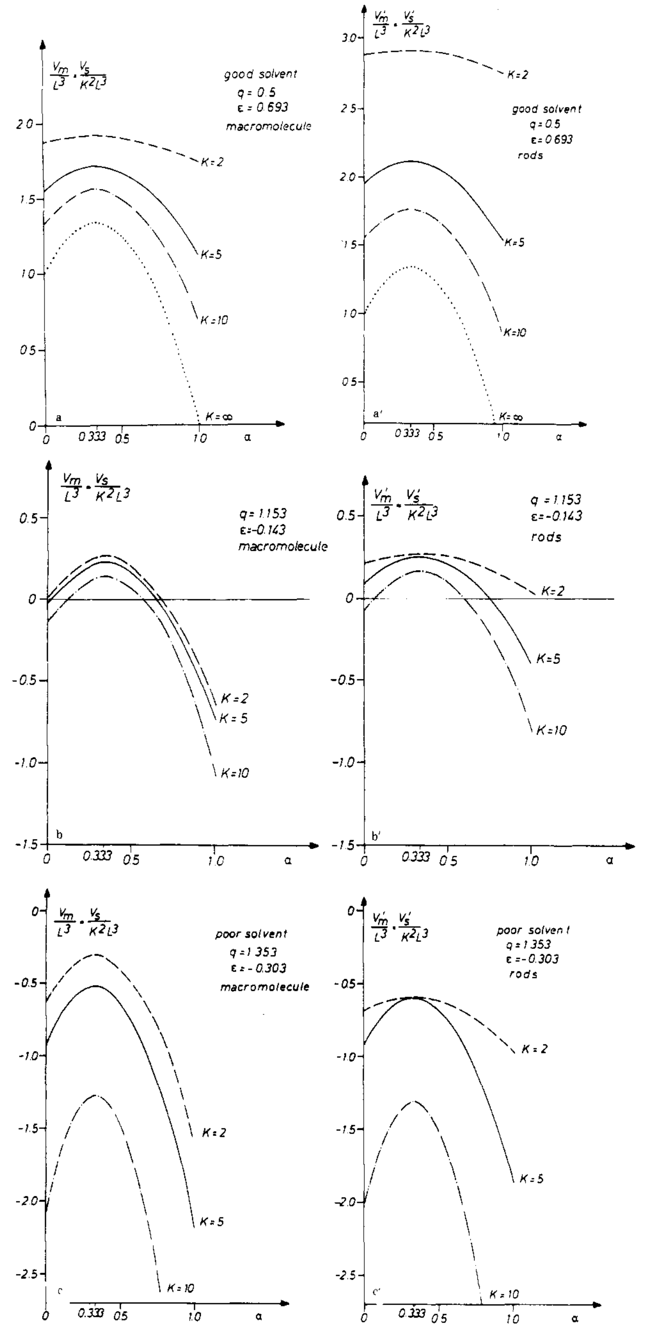

Figure 2. Excluded volume per monomer as a function of segment orientation α and different segment lengths KL for good solvent (a, a′), poor solvent (c, c′), and a solvent near the Θ-state (b, b′): (a, b, c) macromolecular model; (a′, b′, c′) two-rod model.

For the excluded volume of the segment in our macromolecular model we obtain from I, II, and IV

$$\frac{v_s}{L^3} = \left[\alpha(1-\alpha) + \frac{1-\alpha^2}{2}\right]\{K^2 + 2K^2(1-q)\} + \left[\alpha^2 + \frac{(1-\alpha)^2}{2}\right]\left\{8K - \frac{4(1-q^K)(1+q)}{1-q}\right\} \quad (3)$$

It is easy to show by substituting $\alpha = {}^1/_3 + \beta$ and $\alpha = {}^1/_3 - \beta$ into eq 2 and 3 that for any K, q, and β we have

$$v_s'(K, q, \alpha = {}^1/_3 + \beta) = v_s'(K, q, \alpha = {}^1/_3 - \beta)$$

$$v_s(K, q, \alpha = {}^1/_3 + \beta) = v_s(K, q, \alpha = {}^1/_3 - \beta)$$

So, v_s' and v_s are symmetrical of α with regard to $\alpha = {}^1/_3$.

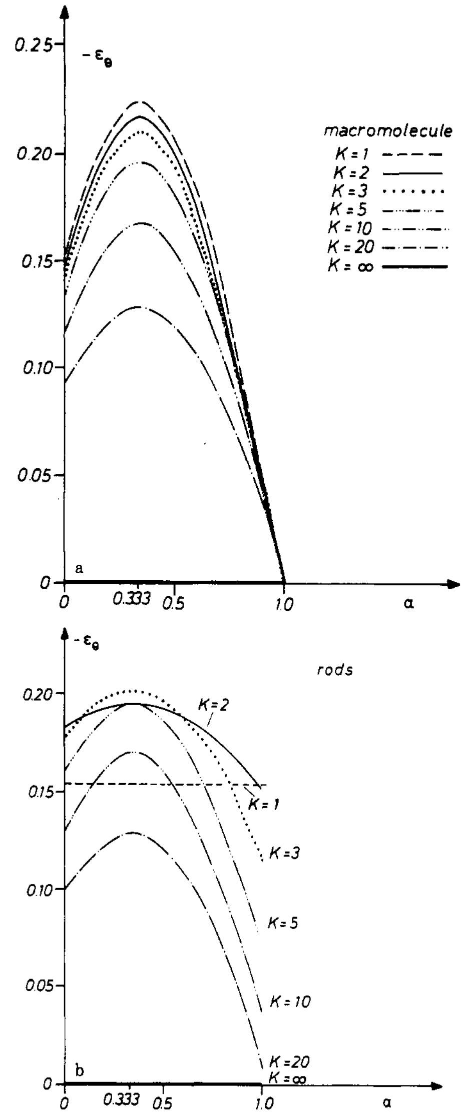

Figure 3. Θ-state for "macromolecular" model (a) and for the two-rod model (b) as a function of segment orientation α for different segment lengths KL.

Results and Discussion

In Figure 2 typical examples of the results are shown for a good solvent (Figure 2a,2a′), for a poor solvent (Figure 2c,2c′), and for a solvent near the Θ-point (Figure 2b,2b′). In spite of very different areas of v_m, all six curves look quite similar. We have maxima in the excluded volume for $\alpha = {}^1/_3$. The excluded volume diminishes symmetrically about $\alpha = {}^1/_3$. Due to segment orientation, the solvent always becomes effectively "poorer" than without segment orientation. The greater is the orientation, the "poorer" becomes the solvent.

In Figure 3 the Θ-state as a function of α for different K for both our models ($v_s = 0$ or $v_s' = 0$) is seen. Excepting for small K, we have qualitatively the same picture for $v_s' = 0$ and $v_s = 0$. ϵ_Θ becomes smaller in absolute value with growing K for all α. When $\alpha = {}^1/_3$, we always obtain a maximum in absolute value of ϵ_Θ (excepting for the trivial situation of a cube, obviously having the Θ-state independent of α). The majority of the polymer–solvent system becomes "better" with increasing temperature and "poorer" with decreasing temperature. Our prediction for such a system with an "upper miscibility point" is that the Θ-temperature grows due to orientation. The greater the orientation, the higher is the Θ-temperature. Summarizing, our work predicts a decrease in excluded volume and an increase in Θ-temperature due to any kind of segmental interaction.

The symmetry of our results for the unoriented situation $\alpha = {}^1/_3$ is of course a consequence of our very symmetrical segment model. Despite its extraordinary symmetry, we hope that our model at least qualitatively describes a broad class of real macromolecules. In addition to real macromolecules having symmetrical segments, this model seems to be true for atactic polymers, because the random distribution of isomers becomes effectively quite symmetrical.

Acknowledgment. In author is indebted to Prof. Dr. R. G. Kirste for valuable discussions and critical reading of the manuscript.

References and Notes

(1) Yamakawa, H. "Modern Theory of Polymer Solutions"; Harper and Row: New York, 1971.
(2) Flory, P. J. "Statistical Mechanics of Chain Molecules"; Interscience: New York, 1969.
(3) Lindner, P.; Oberthür, R. G. *Colloid Polym. Sci.* **1985**, *263*, 443.
(4) Isihara, A. "Statistical Physics"; Academic Press: New York, 1971.
(5) Isihara, A. *J. Chem. Phys.* **1951**, *19*, 397.
(6) Birshtein, T. M.; Skvortsov, A. M.; Sariban, A. A. *Macromolecules* **1976**, *9*, 892.
(7) Onsager, L. *Ann. N.Y. Acad. Sci.* **1949**, *51*, 627.

Thermodynamics of Sorption in Glassy Poly(vinyltrimethylsilane)

Yu. P. Yampolskii,* N. E. Kaliuzhnyi, and S. G. Durgarjan

Institute of Petrochemical Synthesis, Academy of Sciences of the U.S.S.R.,
Leninsky Prospect 29, 117912, GSP-1, Moscow V-71, U.S.S.R. *Received December 19, 1984*

ABSTRACT: Sorption thermodynamics in poly(vinyltrimethylsilane) (PVTMS) was studied with inverse gas chromatography. For various solutes (aliphatic and aromatic hydrocarbons, alcohols, and SO_2) the retention diagrams were found to be linear in the whole temperature range studied, including the glass transition temperature. This is the result of high diffusivity in PVTMS. It enables one to study bulk sorption and thermodynamic polymer–solute interactions in the glassy region. Enthalpy of solution and excess functions of mixing (ΔG_m, ΔH_m, and ΔS_m) in PVTMS were determined. An extrathermodynamic correlation between ΔH_m and ΔS_m was found along with an isoequilibrium constant $\beta = 410$ K. Thermodynamics of sorption in PVTMS, as well as other glassy polymers, is characterized by large negative values of ΔH_m and ΔS_m and a wide variation of ΔH_m and ΔS_m with solute dimensions. These results are in agreement with the predictions of a dual sorption model for glassy polymers. The dimension of a cavity (Langmuir adsorption site) in PVTMS was obtained.

Introduction

Studies of organic solute sorption in polymers using inverse gas chromatography (IGC) have shown[1-3] that in the vicinity of the glass transition temperature (T_g) diffusion limitations in most "polymer–solute" systems prevent establishment of sorption equilibrium in the bulk polymer. According to ref 3, at temperatures $T < T_g$ the method of IGC permits one to study adsorption on the polymer surface, while at temperatures $T \gg T_g$ it measures mainly bulk sorption. The temperature region in the vicinity of T_g corresponds to the nonequilibrium sorption and gas chromatography. Hence, the study of sorption thermodynamics in polymers using IGC is limited to temperatures in excess of $T_g + 50$ °C and sometimes to temperatures as high as 120 °C above T_g.[3] Thus the temperature range of the glassy state and the region of the glass transition, both very important from theoretical and practical points of view, are inaccessible for sorption thermodynamics study by the IGC method.

Later, however, the following studies showed that this was not always the case. First it was demonstrated that in some polymers retention proceeds exclusively by a surface adsorption mechanism even at temperatures above T_g.[4] Later for the system *n*-butyl alcohol–poly(*N*-isopropylacrylamide) (PNIPAM) it was reported[5] that bulk sorption retention has been found both below and above T_g. Bulk sorption retention has been established for IGC of *n*-alkanes on poly(vinyltrimethylsilane) (PVTMS)[6,7] and for some solvents in aromatic polysulfones (PSF).[8]

In the present paper the sorption of different classes of solutes (alkanes, naphthenes, aromatics, alcohols, and SO_2) in PVTMS is investigated below and above the glass transition temperature (170 °C) of this polymer, and the excess thermodynamic functions of mixing are determined.

Table I
Column Parameters[a]

N	loading, mass %	mass of polymer, g	length, m
1	0	0	2.0
2	4.6	0.150	1.5
3	7.0	0.240	1.7
4	11.8	0.211	1.0
5	19.3	0.305	1.0
6	21.2	0.799	2.0

[a] PVTMS. Solvent, benzene, Inert support, Chromosorb W AW DMCS 30/60 mesh; 0.3-cm column diameter.

Experimental Section

The technique has been described previously.[6,7] The characteristics of the basic columns are given in Table I. To cover a wider temperature range for different solutes we varied the length of the columns and therefore the weight of the polymer phase, maintaining a constant concentration of polymer on the carrier. The number of columns actually used was greater than that shown in Table I.

PVTMS, with a molecular weight of about 5×10^5, was obtained by anionic polymerization, initiated by *sec*-butyllithium at a temperature of about 70 °C.

The data[9,10] for the vapor pressures of solutes $p_1°$ at different temperatures were used when determining coefficients at infinite dilution. The second virial coefficients B_{11} and the molar volume of a solute[12] V_1 at various temperatures were used for calculating the corrections for gas-phase nonideality.

While studying different types of solutes we had some problems with the choice of the source of B_{11} values. For some solutes there are direct values. But for others only B_{11} values obtained with correlations or the group contribution approach are available. Since a comparison of various solutes at different temperatures was the main goal of this study, we needed the same accuracy of correction for all the $(a_1/w_1)^\infty$ values. Therefore, a single source of B_{11} values, namely the Berthelot equation,[11] was used. We

0024-9297/86/2219-0846$01.50/0